

# Synthesis and Characterization of ZnO Nanoparticles Derived from Biomass (*Sisymbrium Irio*) and Assessment of Potential Anticancer Activity

Saima Maher,\* Shazia Nisar, Sania Muhammad Aslam, Farooq Saleem, Farida Behlil, Muhammad Imran,\* Mohammed A. Assiri, Arifa Nouroz, Nadra Naheed, Zarmina Azad Khan, and Parveen Aslam

Cite This: *ACS Omega* 2023, 8, 15920–15931

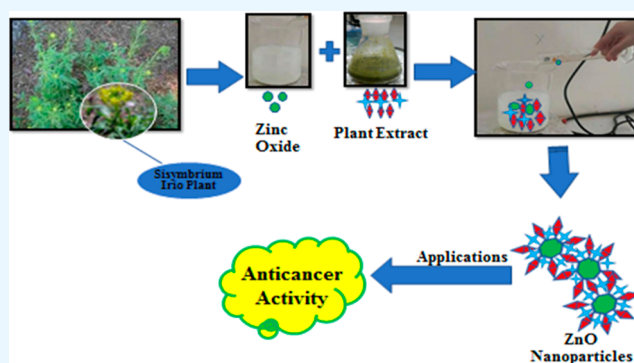
Read Online

ACCESS |

Metrics & More

Article Recommendations

**ABSTRACT:** Cancer treatment development is hampered by chemotherapy side effects, drug resistance, and tumor metastasis, giving cancer patients a gloomy prognosis. Nanoparticles (NPs) have developed as a promising medicinal delivery technique in the last 10 years. The zinc oxide (ZnO) NPs can precisely and captivatingly promote the apoptosis of cancer cells in cancer treatment. There is also an urgent need to discover novel anti-cancer therapies, and current research suggests that ZnO NPs hold significant promise. ZnO NPs have been tested for phytochemical screening and in vitro chemical efficiency. The green synthesis method was employed for the preparation of ZnO NPs from *Sisymbrium irio* (L.) (Khakshi). An alcoholic and aqueous extract of *S. irio* was prepared using the Soxhlet method. Various chemical compounds were revealed in the methanolic extract through qualitative analysis. The results of quantitative analysis showed that the total phenolic content has the highest amount (42.7861 mgGAE/g), while the resultant amounts of (5.72175 mgAAE/g) and (15.20725 mgAAE/g) were obtained in total flavonoid content and antioxidant property, respectively. ZnO NPs were prepared using a 1:1 ratio. The synthesized ZnO NPs were identified to have a hexagonal wurtzite crystal arrangement. The nanomaterial was characterized by scanning electron microscopy, transmission electron microscopy, and UV–visible spectroscopy. The ZnO-NPs' morphology exhibited an absorbance at 350–380 nm. Furthermore, different fractions were prepared and assessed for anticancer activity. As a result of this anticancer activity, all fractions exhibited cytotoxic activity against both BHK and HepG2 human cancer cell lines. The methanol fraction showed the highest activity of 90% (IC<sub>50</sub> = 0.4769 mg/mL), followed by the hexane fraction that showed 86.72%, ethyl acetate showed 85%, and chloroform fraction showed 84% against BHK and HepG2 cell lines. These findings suggested that synthesized ZnO-NPs have anticancer potential.



## 1. INTRODUCTION

In many instances, inorganic materials such as metals and metal oxides are preferable than biological ones due to their durability.<sup>1</sup> Among metal oxides, zinc oxide nanoparticles (ZnO NPs) have generated the greatest reflection as an anticancer agent. It has been found from studies that ZnO NPs cause cytotoxicity to many types of cells. A biotechnological method having a wide range of applications, including medicine and the environment, is nanotechnology. The scientific community is motivated to assess the toxicity of these technologies because of the promise outcomes of nanotechnology research, particularly in the treatment of chronic diseases like cancer.<sup>2</sup> In general, algae, fungus, and various plants are used in the synthesis of nanoparticles.<sup>3</sup> Plant-based synthesis is more useful for the synthesis of nanoparticles, [Table 1](#).

**Table 1. Result of Alkaloids in *S. irio***

| Plant        | Alkaloid |
|--------------|----------|
| 5 g of plant | 0.264 g  |

Typically, plant parts such as the leaf bark, root, stem, seed, flower, fruit, and tubers have been employed to synthesize nanoparticles.<sup>4</sup> Many researchers prefer plants for the synthesis

**Received:** November 29, 2022

**Accepted:** March 30, 2023

**Published:** April 25, 2023



of metal nanoparticles due to their rich source of bioactive phyto-chemical constituents, as well as the availability for immediate use.<sup>5</sup> The plant chemical constituents' act as capping, as well as reducing agents, for the synthesis of nanoparticles. Previously, several attempts have been made for the synthesis of Ag NPs using extracts of plants like *Dodonaea viscosa*,<sup>6</sup> *Gloriosa superba*,<sup>7</sup> *Salvia spinosa*,<sup>8</sup> *Mukia scabrella*,<sup>9</sup> and *Syzygium alternifolium*.<sup>10</sup> Ancient humans used extracts from diametrically opposed medicinal plants to treat a wide range of dreadful diseases, as well as to reduce physical illness and ill health. The medicinal plants have the possession of the medical asset and acquire the beneficial curative personal estate on the body. The medicinal plants are thought to be a rich source of chemical constituents for the invention and modification of drugs. There are about 6000 wild plants species found in Pakistan, and approximately, the medicinal importance of around 400–600 species are reported.<sup>11</sup>

There are many uses of the Cruciferae family in folk medicines, and one of the members of the Cruciferae family reported in the pharmaceutical field is *Sisymbrium irio* Linn. It has approximately 338 genera and nearly 3709 species,<sup>12</sup> which is inclusive of those dispersed worldwide and in Pakistan. *S. irio*, also known as London rocket in English, Khubha in Arabic, and Shaba, Khubkalan, and Khaksi in Urdu,<sup>13</sup> is an annual herb that is specifically found in open deserts, wild fields, on roadsides, in areas of vehicle staging off-highway, on waste places, in pastures, in orchards, and in watering sites of livestock. By reviewing the literature, the perspective shows that *S. irio* is used widely in folk medicine<sup>14</sup> in order to cure inflammation, rheumatoid, and voice disorders and as a febrifuge.<sup>15</sup> It is utilized in the treatment of chest congestion and coughs.<sup>16</sup> It is used to detoxify the spleen and liver, clean wounds, and reduce swelling.<sup>17</sup> *S. irio* is also traditionally used for the vascular, airway disorders and viduals of the gastrointestinal tract.<sup>18</sup> Moreover, its leaves and seeds possess antipyretic, analgesic, and antibacterial characteristics.<sup>19</sup> Merely the seeds of this angiosperm have been used as a medicament, laxative, cardio-tonic, febrifuge, aphrodisiac, hepato-protective, lubricating substance, diuretic, rubefacient, and anti-asthmatic.<sup>20</sup> The phytochemical analyses have shown that S.I has contained many secondary metabolites like alkaloids, flavonoids, oils, glycoside, anthraquinones, and steroids.<sup>21</sup> Antioxidant, anti-microbial, analgesic, antipyretic, antifungal,<sup>22</sup> antibacterial, and cytotoxic activities have been reported.<sup>23,24</sup>

The targeted administration of nanomedicine has heightened interest in its potential in cancer treatment in recent years, high absorption, biocompatibility, and multifunctionality of the generated nanoparticles.<sup>25</sup> The primary justification for this work is that it is critical to use the ZnO-based system to treat aggressive and phenotype type cancer, it is distinguished by a considerable increase in metastasis, a poor prognosis, and unpredictability in therapy because conventional chemotherapy reduces malignant cells.<sup>25,26</sup> Ionic zinc is required for immune function, homeostasis, oxidative stress, apoptosis, and aging, as well as other biological disease cycles.<sup>27</sup> As it influences cellular metabolism and gene expression cancer cell death, Zn<sup>2+</sup> has an impact on cancer and is an intriguing chemical therapy.<sup>28–30</sup>

The main benefit of nanomaterials is the capacity to create controlled nanoparticles smaller than 100 nm. An optical visible electrical and semiconductor with a high energy (60 meV) and an inclusive range of 3.37 eV at room temperature is zinc oxide (ZnO).<sup>31</sup> It also has a strong direct band difference. When cancer cell selection is high, ZnO NPs harm cancer cells more than healthy cells.<sup>32</sup> Recently, ZnO NPs were supposed to have a

highest level of cancer cell selectivity in addition to therapeutic proportions compared to chemotherapeutic drugs.<sup>33</sup> ZnO NPs have been utilized to suppress UV radiation due to their low toxicity and biodegradability,<sup>34</sup> and it has been reported to be used for anti-diabetic activity,<sup>35,36</sup> antimicrobial agent,<sup>37</sup> anti-inflammatory agent,<sup>38</sup> wound healing,<sup>39</sup> cancer imaging and diagnosis,<sup>40</sup> photocatalysis,<sup>41</sup> and electronics.<sup>42</sup>

Green synthesis has recently emerged as an alternate method of fabricating nano-metal oxides, the most commonly used being ZnO (zinc oxide). As a result, biological synthesis methods were employed to generate ZnO NPs with minimal environmental impact.<sup>42</sup> This approach has numerous advantages, including environmental friendliness due to the reduction of hazardous byproducts, biocompatibility, immunogenicity, cost-effectiveness, ease of scaling up, easiest in laboratory procedure, and the production of safe-to-use NPs. UV radiation can be quickly absorbed by a ZnO NP.<sup>43</sup> Zinc is a major cofactor in various biological pathways and plays a crucial role in maintaining cell homeostasis; thus, ZnO is biocompatible. The ZnO given is quickly biodegradable or can engage in the body's active nutritional process. In comparison to other metal nanoparticles, ZnO NPs are naturally effective cytotoxic against in vitro cancer cells.<sup>44,45</sup> Although extracellular ZnO is benign, higher intracellular ZnO concentrations suggest an increase in cytotoxicity via zinc-mediated protein synthesis mismatch and oxidative stress.<sup>46,47</sup> In this paper, we report a one-step method scheme that uses a greener, environmentally friendly, harmless, and safer methodology to generate mono disperse ZnO-NPs by using the whole extract of *S. irio* (L.), a plant in a harsh environment comprising highest quantities of chemical constituents,<sup>48</sup> controlling the generated NPs' shape and size. Furthermore, the structure of nanoparticles and the various activities of synthesized nanoparticles have been determined.<sup>49</sup> This research exposed a simple methodology for the synthesis of ZnO NPs by the *S. irio* available in the Balochistan region (Quetta) in Pakistan. The advantages of this study are as follows: simplicity, room-temperature process and less time consumption 20 min, reliability, and mass production. As per the present literature and current data, this is probably the first report on the synthesis of ZnO-NPs using the *S. irio* extract. The crystal structures and optical and morphological features of the ZnO-NPs were examined. This discovery could help in the field of medical research by reducing morbidity and death from multidrug-resistant malignancy. Targeted NP therapeutics have great potential for cancer therapy as they provide enhanced efficacy and reduced side effect of cancer available drug.<sup>51</sup>

## 2. MATERIALS AND METHODS

**2.1. Collection of Plant Sample.** *S. irio* (L.) the whole plant was collected during the month of May from the different areas of Chashma Achozai killi Dummaran. It is a mountain area which is located on the airport road in Quetta, Baluchistan. The plant was identified by Ms. Pashtana Sahib Khan, plant taxonomist from the Botany department in Sardar Bahadur Khan Women's University Quetta. The samples have been identified and registered in the botany department record as CHEM-BOT-SI-965. The whole plant was washed with tap water in order to remove the dust and the washed plant material was shade dried for 4 weeks at room temperature and then converted to a fine powder, weighed, and stored for further uses.

**2.2. Chemicals.** The chemicals used were zinc acetate 2-hydrate Zn(CH<sub>3</sub>COO)<sub>2</sub>·2H<sub>2</sub>O, methanol (CH<sub>3</sub>OH), sodium hydroxide (NaOH), ethanol (CH<sub>3</sub>CH<sub>2</sub>OH), and distilled water.

**Table 2. Phytochemical Analysis of Metanolic Extracts of *S. irio***

| S.No | phytochemicals     | chemical Tests            | test procedure   | observations              | result |
|------|--------------------|---------------------------|--|---------------------------|--------|
| 1    | alkaloids          | (a): Mayer test           | 2 mL of filtrate + Mayer reagent                               | white creamy precipitate  | +      |
|      |                    | (b): Wagner test          | 2 mL of filtrate + Wagner reagent                              | reddish brown precipitate | +      |
| 2    | amino acid         | ninhydrin test            | Filtrate + 2 drops of ninhydrin solution                       | purple color              | +      |
| 3    | carbohydrates      | (a): Molisch test         | Filtrate + alpha naphthol + sulfuric Acid                      | violet Color              | +      |
|      |                    | (b): Benedict test        | 0.5 mL of Filtrate+0.5 mL of Benedict reagent + heat for 2 min | brown Color               | +      |
| 4    | fixed oil and fats | spot test                 | Small quantity of extract + Filter paper                       | oil stain on the paper    | +      |
| 5    | glycosides         | flame test                | Small quantity of extract on glassrod + flame                  | extract burn like a sugar | +      |
| 6    | phenolic compound  | (a): ferric chloride test | 2 mL filtrate + few drops of ferric chloride                   | dark green color          | +      |
|      |                    | (b): lead acetate test    | Filtrate + few drops of lead acetate                           | bulky white precipitate   | +      |
| 7    | flavonoids         | alkaline reagent test     | Filtrate + ammonium hydroxide solution                         | yellow fluorescence       | +      |
| 8    | saponins           | foth test                 | Few mL filtrate + shake for 2–5 min                            | No Foam                   |        |

**2.3. Phytochemical Analysis.** The medicinal plant *S. irio* can be allotted to the diverse nature of phytochemicals formed by the plant. The current study contracts with the assessment of total alkaloid content (TAC), total flavonoid content (TFC), total phenolic content (TPC), and antioxidant capacity of the *S. irio* extract. The spectrophotometric determination of TPC was done by using the Folin–Ciocalteu (FC) procedure, and the antioxidant capacity was determined by using the ammonium molybdate method. The antioxidant capacity was estimated using concentrated ammonium hydroxide (NH<sub>4</sub>OH) solution, and TFC was estimated by using 2% solution of aluminum trichloride (AlCl<sub>3</sub>).

**2.4. Detection of Total Alkaloid Content.** 5 g of plants' powdered form was taken in a 500 mL beaker. Ethanol solution was added until all the powdered plant was dipped in it and then 200 mL of 10% CH<sub>3</sub>CO<sub>2</sub>H was added to the plant solution. The mixture could stand for 24 h and then filtered. The filtrate was kept in a boiling water bath at 60 °C until the volume became 1/4 of the original volume. Then, concentrated NH<sub>4</sub>OH was added to the solution of plant sample and the solution could stand until the precipitates are formed and then filtered through a filter paper. Then, the filter paper could dry and weigh the alkaloids.<sup>21</sup> The procedure was repeated twice to ensure the accuracy of the average quantity.

**2.5. Estimation of Total Phenolic Contents.** The previously designated simple and modified method is used for determining the TPC in plants.<sup>50</sup> Consider adding 1 mL of the FC chemical to three test tubes containing 2 mL of the test material each. After incubating the test tubes for 25 min, 0.8 of sodium carbonate was added to the reaction mixture. Following the triple performance, the absorbance of each reaction mixture was measured at 765 nm using gallic acid as the standard.<sup>41</sup>

**2.6. Estimation of Total Flavonoid Content.** The TFC was determined using the aluminum chloride colorimetric method recommended by<sup>52</sup> with minor changes based on system appropriateness. 0.6 mL of 2% aluminum chloride was added to the test samples (2 mL from 0.25 g/100 mL methanol) and incubated for 60 min. Subsequently, following the addition of 1.0 M potassium acetate, 160 μL of distilled water was added. For 30 min, the resultant combination was maintained at room temperature. At 415 nm, the absorbance was measured.<sup>52</sup> The experiment was repeated three times to determine the precise absorbance.

**2.7. Antioxidant Capacity Assay.** The total antioxidant capacity of the extracts and fractions based on ammonium molybdate was measured succinctly by combining 2 mL of each test sample and positive control (ascorbic acid, 1 mg/mL) with 1 mL of reagent (1 mL of sulfuric acid, 1 mL of sodium phosphate

solution, and 1 mL of ammonium molybdate). A typical blank solution contained 1 ml of the reagent solution and the appropriate volume of the same solvent used for each sample. Test tubes were incubated for 95 min at 95 °C in a hot water bath. After cooling at room temperature, 200 μL of all samples were transferred to 96-well plates, and the absorbance at 650 nm was measured.<sup>53</sup> The antioxidant activity was expressed as the number of μg equivalents of ascorbic acid per milligram extract, that is, μg AAE/mg extract as stated by.<sup>54</sup>

**Table 3. TPC, TFC, TAC, and Antioxidant Capacity of *S. irio* L**

| assay                | result                         |
|----------------------|--------------------------------|
| TPC                  | 42.7861 mg of GA/g of extract  |
| TFC                  | 5.72175 mg of AA/g of extract  |
| TAC                  | 0.264 g                        |
| antioxidant capacity | 15.20725 mg of AA/g of extract |

**2.8. Biosynthesis of Zinc Oxide Nanoparticles.** The precipitation process was used to synthesize zinc oxide nanoparticles. In 100 mL of distilled water, 10 g of powdered plant material was dissolved. At 60 °C, the solution was heated and then cooled. This process was repeated thrice, and then, the mixture was kept at room temperature overnight. After that, the mixture which was filtered three times through the Buchner funnel by using Whatman filter paper NO.1 and 100 mL of filtrate was obtained. Plant extract and sodium hydroxide (NaOH) solution were used as reducing and stabilizing agents, while zinc acetate Zn(CH<sub>3</sub>COO)<sub>2</sub> molar solution was used as a precursor salt, which was used for the synthesis of ZnO NPs. NaOH was added dropwise to the Zn (CH<sub>3</sub>COO)<sub>2</sub> solution with continuous stirring to get a basic solution of 12 pH. 10 mL of the plant filtrate was added to the basic solution and the solution was heated for 3 h. Then, fresh UV of the solution sample was measured with the help of a UV spectrophotometer. Once the reaction mixture confirmed, the ZnO NPs form. Then, the solution was kept in the refrigerator overnight. Afterward, a solid residue was observed in the container, the water was discarded, the pellets were washed, centrifuged 2–3 min in a centrifuge machine having 15000 rpm, and washed twice with distilled water and once with ethanol to remove impurities. After washing with the ethanol, the pellets were collected in the Petri dish, and then, it was kept in the oven for 4 h at 70 °C to obtain the dry powder.

**2.9. Characterization of ZnO NPs.** There are several analytical techniques like Fourier transform infrared (FT-IR) spectroscopy, scanning electron microscopy (SEM), and X-ray

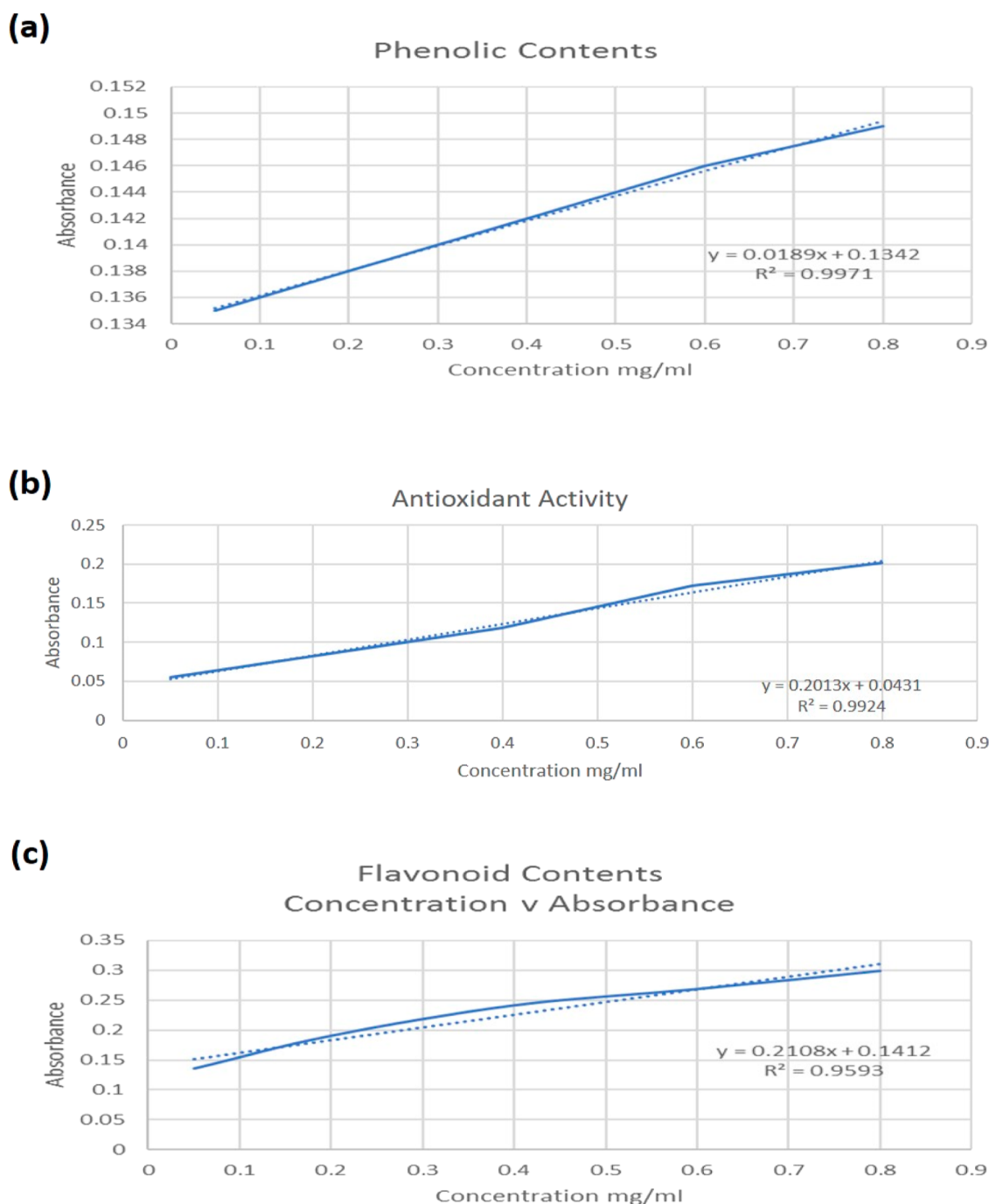


**Figure 1.** Results of (a) phenolic contents, (b) antioxidant activity, and (c) flavonoid contents.

diffraction (XRD), and they were used to analyze the nature, chemistry, and morphology of the synthesized NPs. The FT-IR spectroscopy with the range of 500–4000  $\text{cm}^{-1}$  was appropriate for the information about identification of the molecular components. The dried powder of ZnO NPs was also subjected to the analysis. The XRD technique is used to determine the phase of a crystalline material and to calculate the size of NPs. Meanwhile, the surface topography and compositions of ZnO NPs were analyzed with the help of SEM.

**2.10. Anticancer Activity: Preparation of Stock Solution.** *S. irio* ZO-NPs 5 mg is dissolved in 1 mL of DMSO (dimethyl sulfoxide) with constant stirring to form a 5 mg/mL homogenized stock solution.

**2.10.1. Cell Line Sampling.** The normal cell line BHK (Baby hamster kidney cell line) and the malignant cell line HepG2 (hepatocellular carcinoma cell line) were employed in the experiment. Both cell lines were obtained from the CRIMM department at the University of Lahore. For preservation, cell lines were frozen in liquid nitrogen in cryovials and maintained revitalizing throughout the operation.

**2.10.2. Culturing of Cell Lines.** The cryovials containing frozen cells were thawed in the cell culture facility at the University of Lahore. These thawed cell lines were then seeded in culture flasks with Dulbecco's modified Eagle medium–high glucose (DMEM-HG), 10% (v/v) fetal bovine serum (FBS), 100 units/mL streptomycin, and 100 g/mL penicillin. The cryovials

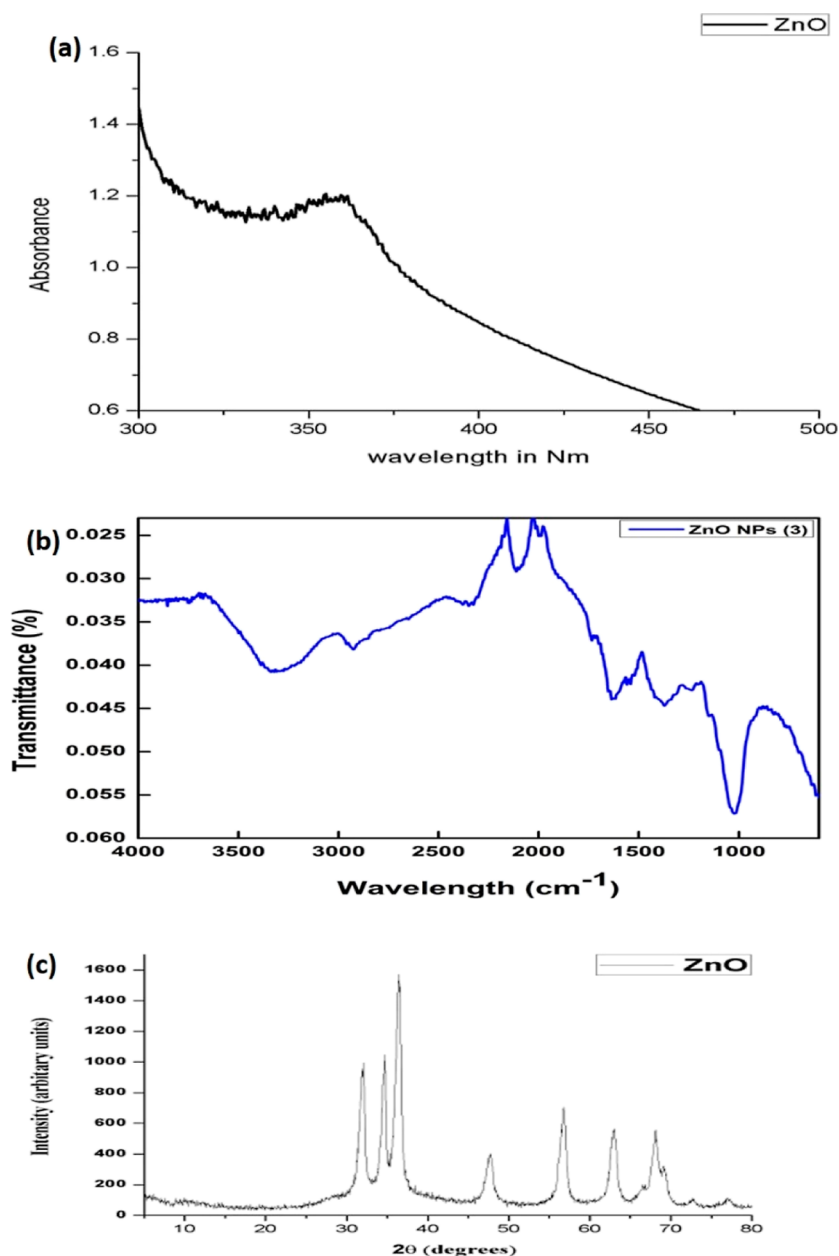


**Figure 2.** UV-vis spectra (a), FTIR results (b), and XRD (c) patterns of ZnO NPs of *S. irio*.

containing frozen cells were thawed in the cell culture facility at the University of Lahore. These thawed cell lines were then seeded in culture flasks with DMEM-HG, 10% (v/v) FBS, 100 units/mL streptomycin, and 100 g/mL penicillin.<sup>31</sup> When seeded cells with HepG2 and BHK cells reached 70–80% confluency, they were rinsed with normal saline and treated for 5 min with trypsin–EDTA (ethylene-diamine-tetra acidic corrosive). Cells were centrifuged at 2000 rpm for 5 min after meticulous microscopic examination. The resilient was taken from the centrifuged mixture and the pellet was reassembled.

**2.10.3. Treatment of Cell Lines with Plant Extract.** *S. irio* ZnO NPs were treated using both the BHK and HepG2 cell lines. Treatments were given to the HepG2 cell line at dosages of 0.250, 0.500, 1.000, and 2.000 mg/mL. The IC<sub>50</sub> was calculated at numerous doses since 2.000 mg/mL resulted in a fatality rate greater than 50%. The IC<sub>50</sub> concentration was then applied to the BHK cell line to determine viability. The 3-(4, 5-dimethylthiazol-2-yl)-2, 5-diphenyltetrazolium bromide MTT

test was performed on both BHK and HepG 2 cell lines. One group was made for the HepG2 cell line and one group was made for the BHK cell line.

**2.10.4. Cytotoxicity Assay.** Assay of (4, 5-dimethylthiazol-2-yl)-2, 5-diphenyltetrazolium bromide (MTT) was accomplished on both cell lines and then cultured in a 96-well plate. To examine cell cytotoxicity, the monolayer of cultured cells were treated with phosphate-buffered saline (PBS) (Invitrogen Inc., USA) and then incubated in 100 μL of complete medium comprising 25 μL of MTT solution (Invitrogen Inc., USA) for 24 to 48 h. The MTT was transformed to purple colored formazan crystals in living cells, which were then solubilized with dimethyl sulfoxide (DMSO) (Invitrogen Inc., USA). Absorbance of solutions was measured at 570 nm with an ELISA reader.

Table 4. Anticancer Activity of *S. irio*

| extracts         | concentrations | % viability | mean abs | IC <sub>50</sub> |
|------------------|----------------|-------------|----------|------------------|
| M = 1            | 0.250 mg       | 20.61185    | 26.04855 | 0.13024 mg/mL    |
|                  |                | 41.95166    |          |                  |
|                  |                | 15.58214    |          |                  |
|                  | 0.500 mg       | 23.68069    | 31.36656 |                  |
|                  |                | 28.65264    |          |                  |
|                  |                | 41.76635    |          |                  |
|                  | 1.000 mg       | 19.29254    | 37.45013 |                  |
|                  |                | 37.55148    |          |                  |
|                  | 2.000 mg       | 55.50638    | 57.71104 |                  |
|                  |                | 74.41683    |          |                  |
|                  |                | 46.09669    |          |                  |
|                  | ETH = 2        | 0.250 mg    | 52.61962 |                  |
| 32.80593         |                |             |          |                  |
| 86.3026          |                |             |          |                  |
| 0.500 mg         |                | 53.79984    | 46.59121 |                  |
|                  |                | 50.00478    |          |                  |
|                  |                | 30.65801    |          |                  |
| 1.000 mg         |                | 59.11085    | 83.32684 |                  |
|                  |                | 87.5239     |          |                  |
| 2.000 mg         |                | 82.63205    | 36.69357 |                  |
|                  |                | 79.82456    |          |                  |
|                  |                | 28.79541    |          |                  |
| CH = 3           |                | 0.250 mg    | 58.84512 | 74.32446         |
|                  | 22.44019       |             |          |                  |
|                  | 53.29828       |             |          |                  |
|                  | 0.500 mg       | 91.40555    | 86.96488 |                  |
|                  |                | 78.26954    |          |                  |
|                  |                | 94.16826    |          |                  |
|                  | 1.000 mg       | 88.13787    | 65.73454 |                  |
|                  |                | 78.58852    |          |                  |
|                  | 2.000 mg       | 48.85277    | 59.88109 |                  |
|                  |                | 87.82453    |          |                  |
|                  |                | 60.52632    |          |                  |
|                  | Z = 5          | 0.250 mg    | 60.27725 | 79.19669         |
| 60.47449         |                |             |          |                  |
| 58.89155         |                |             |          |                  |
| 0.500 mg         |                | 78.53728    | 5.697205 |                  |
|                  |                | 2.49776     |          |                  |
|                  |                | 76.55502    |          |                  |
| 1.000 mg         |                | 7.122371    | 81.49038 |                  |
|                  |                | 1.835273    |          |                  |
|                  |                | 8.133971    |          |                  |
| 2.000 mg         |                | 90.20076    | 56.9766  |                  |
|                  |                | 86.1683j11  |          |                  |
|                  |                | 68.10207    |          |                  |
| untreated        | 0.250 mg       | 56.93117    | 32.23984 | 0.16119mg/ml     |
|                  |                | 55.50582    |          |                  |
|                  |                | 58.49282    |          |                  |
|                  | 0.500 mg       | 5.592734    | 31.80398 |                  |
|                  |                | 88.85407    |          |                  |
|                  |                | 2.272727    |          |                  |
|                  | 1.000 mg       | 5.893881    | 59.45337 |                  |
|                  |                | 47.85139    |          |                  |
|                  |                | 41.66667    |          |                  |
|                  | 2.000 mg       | 48.23136    | 61.90771 |                  |
|                  |                | 85.63115    |          |                  |
|                  |                | 44.49761    |          |                  |
| no concentration | 63.43212       | 100 ± 0.00  |          |                  |
|                  | 58.4154        |             |          |                  |
|                  | 63.8756        |             |          |                  |

Table 4. continued

| extracts  | concentrations | % viability | mean abs | IC <sub>50</sub> |
|-----------|----------------|-------------|----------|------------------|
| untreated |                | 100         |          |                  |
|           |                | 100         |          |                  |

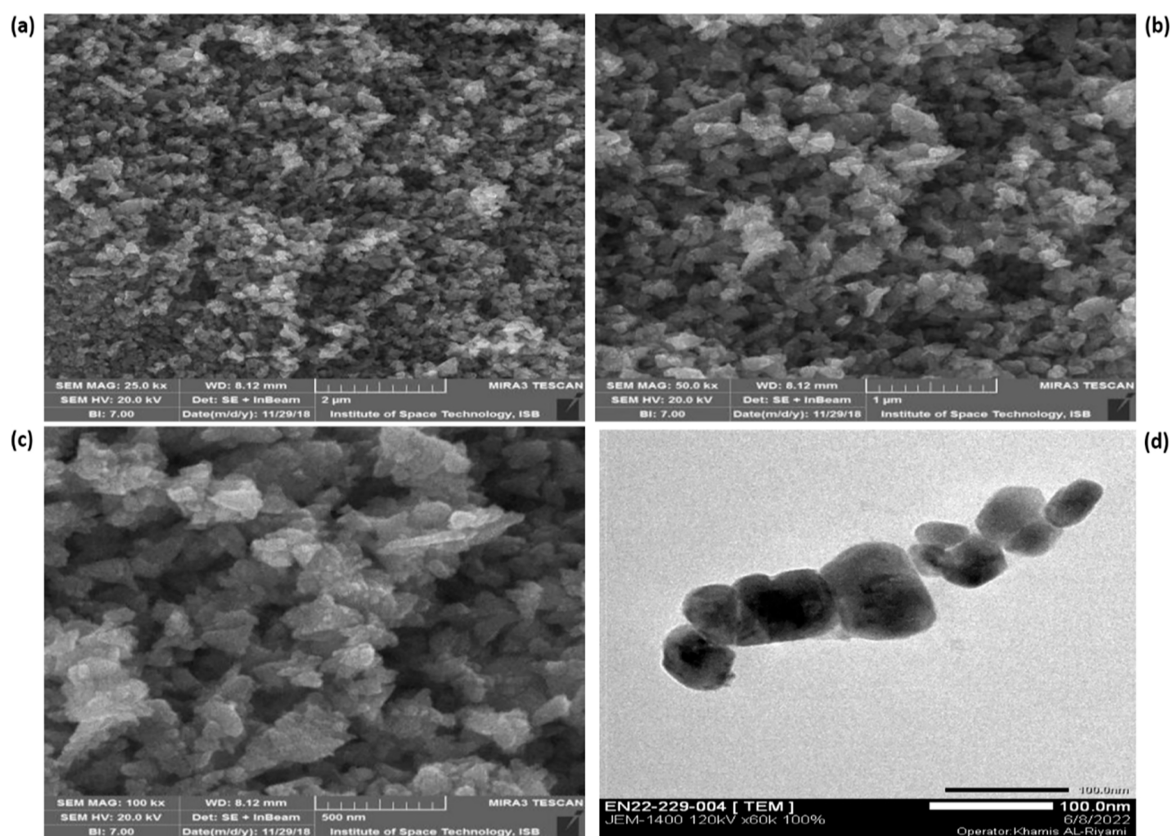
Figure 3. Low- (a), medium- (b), and high-magnification (c) FESEM images and TEM images (d) of ZnO NPs of *S. irio*.

Table 5. % Viability against BHK Cell Line

| name of extracts | concentration | % viability |
|------------------|---------------|-------------|
| untreated        | no treatment  | 100%        |
| M                | Mg            | 90%         |
| ETH              | Mg            | 85%         |
| CH               | Mg            | 84%         |
| H                | Mg            | 86.72%      |
| Z                | Mg            | 99%         |

### 3. RESULTS AND DISCUSSION

**3.1. Flavonoids and Phenolic Acids.** The main active ingredients of *S. irio* include alkaloids, flavonoids, and phenolic acids, which have been found in recent pharmacological investigations to have antioxidant, anti-diabetic, anti-pathogenic microorganism, and anti-cancer potential. The flavonoids, indole, and their derivatives present in *S. irio* plant act as a possible cancer preventive agent,<sup>15</sup> while the phenolic compound, sterol, and alkaloid (nicotine) act as a reducing agent in a single reaction and reduce, cap, and stabilize the Zn metal ions to ZnO-NPs.<sup>23</sup> The synergistic actions of the flavonoid (apigenin) and phenolic acids resulted in ZnO NPs, with the acids functioning as efficient reducing agents (due to their numerous hydroxyl groups) and effective dispersants (due to their derived C, O groups), improving the NPs' stability. The

phenolic derivative has been shown to produce Zn ONPs itself and is regarded as the most important molecule for decreasing ZnO during the production of the plant extract. A method and chemical pathway for producing ZnO NPs are proposed.<sup>16</sup>

**3.2. Phytochemical Screening.** Phytochemical estimate was performed in crude methanolic soluble fractions using established procedures, and the bioactive compounds tested included tannins, alkaloids, steroids, saponins, phenols, and flavonoids, as shown in Table 2. The presence of key phytochemicals such as TPC, TFC, and TAC in the crude methanolic extract of whole parts of *S. irio*, as well as antioxidant potential, might be considered as a favorable indicator for selecting a plant for NP synthesis.

**3.3. Biosynthesis of Zinc Oxide Nanoparticles.** The presence of TPC, TFC, TAC, and antioxidant capacity in the plant extract of *S. irio* as shown in Table 1 revealed that the *S. irio* plant extract can perform a vital role in the biosynthesis of ZnO NPs. The change in color of the basic solution of the precursor salt and sodium hydroxide on mixing *S. irio* plant extract indicated the formation of NPs, and as the reaction proceeded, the solution turned milky white. No further color changed and thickening of the solution revealed the reaction completion. Through centrifugation and washing process, ZnO NPs were isolated and converted into their dried powder form, which was used to confirm the formation of ZnO NPs through various

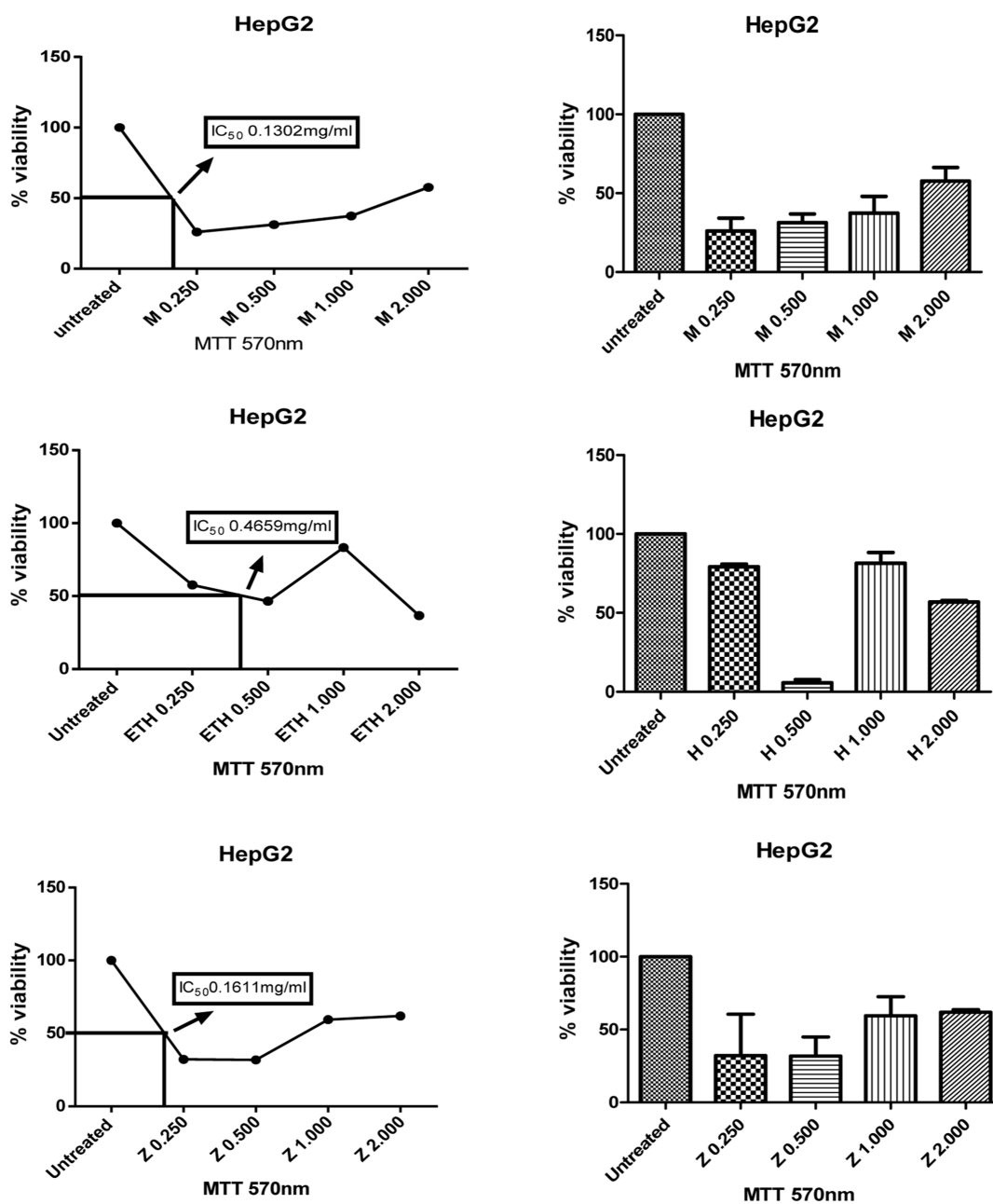


Figure 4. IC<sub>50</sub> of M fraction (a,b), ETH fraction (c,d), and Z fraction (e,f).

techniques. The steps followed for characterization of ZnO NPs are UV–Vis, XRD, SEM, and FT-IR analysis.

**3.4. Total Phenolic and Flavonoid Content.** Gallic acid (0.05, 0.2, 0.4, 0.6, and 0.8  $\mu\text{g}/\text{mL}$ ) (Table 3 and Figure 1) was used as a positive control to create a calibration curve in parallel under the same operating circumstances, and the correlation was found to be significant at the 0.05 and 0.2 level. The data are given as  $\mu\text{g}$  of gallic acid equivalent per milligram of extract ( $\mu\text{g}/\text{ml}$  GAE/mg extract), and the assay was carried out in triplicate.

The calibration curve was obtained using quercetin as a standard at different concentrations of (0.05, 0.2, 0.4, 0.6, and 0.8  $\mu\text{g}/\text{mL}$ ), respectively (Table 3 and Figure 1). The experiment was carried out in triplicate, and the flavonoid concentration was recorded in  $\mu\text{g}$  equivalents of quercetin per milligram extract ( $\mu\text{g}$  QE/mg extract). The calibration curve of  $y = 0.2108x + 0.1412$  ( $R^2 = 0.9593$ ) and the correlation was found to be significant at 0.2 level.

**3.5. Estimation of Antioxidant Capacity.** A calibration curve ( $y = 0.2013x + 0.0431$ ,  $R^2 = 0.9924$ ) of ascorbic acid was drawn at final concentrations of 0.8, 0.6, 0.4, 0.2, and 0.05  $\mu\text{g}/\text{mL}$  (Table 3 and Figure 1) and the experiment was achieved in triplicate. The antioxidant activity was expressed as the number of  $\mu\text{g}$  equivalents of ascorbic acid per milligram extract, that is,  $\mu\text{g}$  AAE/mg extract as stated.<sup>42</sup>

**3.6. UV/Vis Analysis.** The UV/vis spectrum showed the maximum surface plasma resonance absorption of synthesized *S. irio* ZnO NPs in the range of 350–380 nm at alkaline pH 12 (Figure 2). This characteristic absorbance of the peak reveals the formation of ZnO NPs. Because of the characteristic range of the ZnO pure NPs and there is no other peak absorbed in the spectrum, it further confirmed that no other compound is synthesized except ZnO NPs.

**3.7. FTIR Analysis.** The FTIR results of synthesized *S. irio* ZnO -NPs were detected at 3442, 2921, 2353, 1398, 419 and



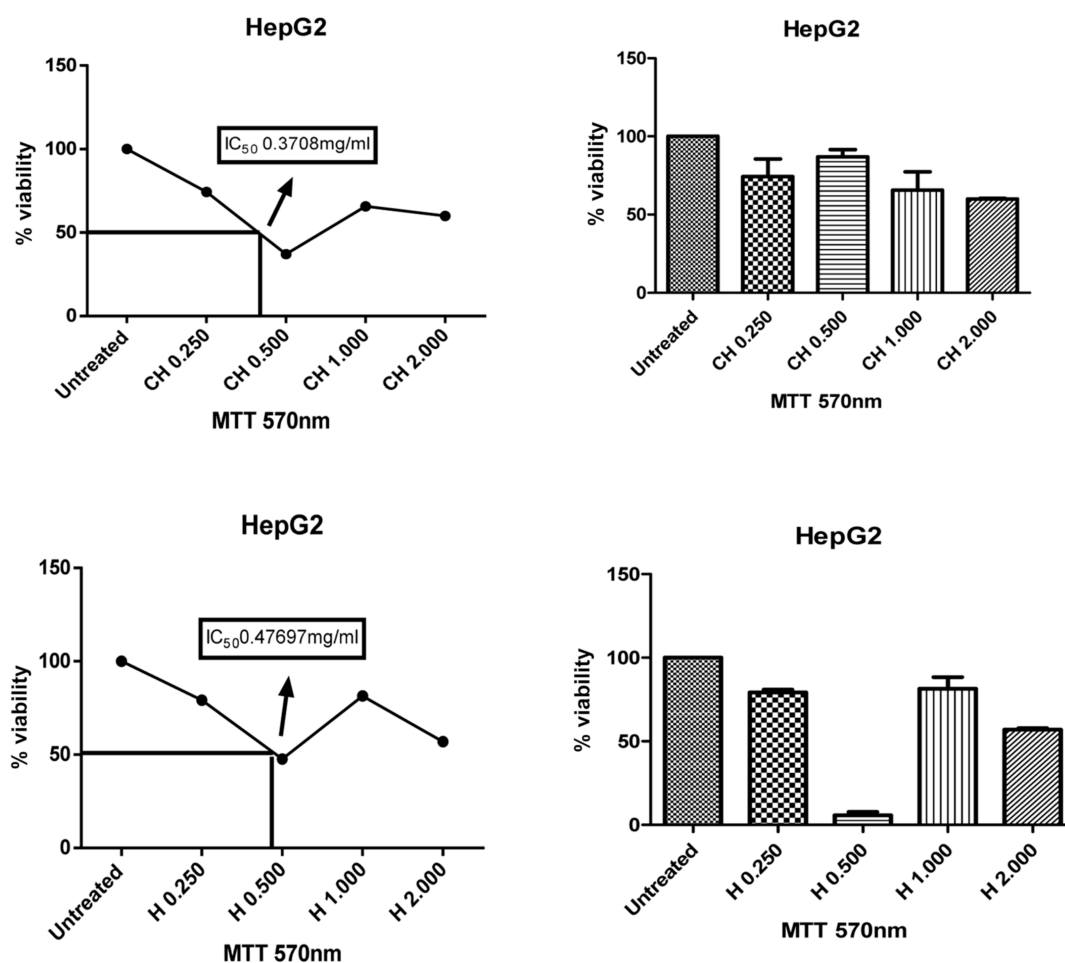


Figure 5. IC<sub>50</sub> of CH fraction (a,b) and H fraction (c,d).

3414, 2345, 1391, and 436 cm<sup>-1</sup> respectively (Figure 2). A broad peak exhibited at 3414 and 3442 cm<sup>-1</sup> in the highest energy state due to strong O–H stretching of the hydroxyl moiety of phenols and alcoholic functionality.<sup>36</sup> The other strong absorption peaks at 2344 and 2363 cm<sup>-1</sup> for the occurrence of CO molecules in the plant extract.<sup>37</sup> The FTIR peak exhibited at 1593 cm<sup>-1</sup> is due to the aromatic C–C stretching ring, and the bending vibrations of the carbonyl group of ketones and aldehydes showed that the strong intensity at 1401 cm<sup>-1</sup> is due to presence  $\alpha$ -CH<sub>2</sub>. The characteristic peak appeared at the region 400 and 600 cm<sup>-1</sup> is assigned to the Zn–O stretching vibration,<sup>38</sup> which was the conformation that ZnO NPs were synthesized by the *S. irio* plant extract.

**3.8. X-ray Diffraction Analysis.** *S. irio* ZnO-NPs were assessed by X-ray diffraction for their crystalline nature. The diffraction pattern showed four main peaks at  $2\theta$  values of 31.8, 34.5, 36.27, 47.5, 56.7, 62.8, and 67.5 (Figure 2). The mean particle size of zinc nanoparticles was calculated using Scherrer's equation: ( $D = K\lambda/\beta \cos\theta$ ), which are mostly relevant for the ZnO structure. Observable line broadening in the XRD peaks indicates that the material which is synthesized is in the nm range.

**3.9. Scanning Electron Microscopy-Energy Analysis.** SEM was used to examine surface morphologies of biosynthesized ZnO NPs, and results are shown in Figure 3. Figure 3a depicts the SEM image of as-generated ZnO NPs synthesized using a 1:1 ratio of reactants by volume. +e picture depicts spherical forms with particles inclined together due to the

presence of a more capping agent that stabilizes the nanoparticles.

**3.10. Transmission Electron Microscopy.** The transmission electron microscopy (TEM) analysis was performed to better recognize crystalline properties and size of the synthesized nanoparticles. The TEM images of ZnO confirmed that the particles are hexagonal with little thickness variation, which matches the SEM results. This figure shows that the majority of the ZnO NPs are hexagonal in form, with typical particle sizes of 100 nm. Our data are compared to previously reported data.

**3.11. Future Perspective.** The objective of the current study was to determine the chemical components of *S. irio* through quantitative and qualitative analysis. The results showed that the plant extract contained a different class of secondary chemical components, including carbohydrates, alkaloids, amino acids, glycosides, phenolic compounds, oils, and fats, with the exception of saponin. According to the polarity of the solvent, methanol was used to extract the entire plant (leaves, flower, stem, and root) using the Soxhlet method. On the basis of polarity, the produced methanolic extract was used to prepare the different fractions (*n*-hexane, chloroform, ethyl acetate, and aqueous extract).

Methanolic extract was used for the phytochemical chemical screening, which included quantitative and qualitative studies to assess the TPC, TFC, and antioxidant activity. The TPCs were estimated according to slightly modified procedure as described previously by.<sup>55</sup> UV–visible spectrophotometry technique was used to determine the antioxidant property<sup>56</sup> as well as TPC and

TFC. The protocol of TFC<sup>57</sup> was followed by the colorimeter, and results of quantitative analysis are 5.72175 mg/AEE/g (total flavonoid content), 15.20725 mg/AEE/g (antioxidant activity), and 42.7861 mg/GAE/g (total phenolic content).<sup>58</sup> The present study revealed that *S. irio* (cruciferae) is a medicinal plant, as it possesses anti-inflammatory, analgesic due to the high flavonoid content, and anti-oxidant activities and can be used for the treatment of such diseases. Furthermore, the TLC (thin layer chromatography) method was used for the standardization of these different fractions, and numerous combinations of mobile phases were tried to get good separation of various compounds present in the *S. irio* plant.

*S. irio* contains a variety of bioactive chemicals such as indoles, phenols, coumarins, amines, flavonoids, isothiocyanates steroids, and glycosides. The anticancer activity was done (methanol, hexane, chloroform, and ethyl acetate). According to the anticancer activity results, all the fractions show a dose-dependent cytotoxic effect against the two cell lines such as BHK and HepG2 cell lines, respectively. A previous research showed the component extracted from hexane extracts of *S. irio* aerial fraction shown significant dose-dependent cytotoxicity action against Vero cancer cell lines.<sup>59</sup> However, the 5.038 g methanol fraction showed the highest activity (90%) ( $IC_{50} = 0.4769$  mg/mL) against BHK and HepG2 cell lines. Next the 7.302 g hexane fraction shows 86.72% activity ( $IC_{50} = 0.4769$  mg/mL), 0.561 g of ethyl acetate shows 85% ( $IC_{50} = 0.4659$  gm/mL), and the 0.348 g chloroform fraction showed 84% ( $IC_{50} = 0.37087$  gm/mL) activity against BHK and HepG2 cell lines (Tables 4 and 5; Figures 4 and 5). The Si-AgNPs demonstrated significant cytotoxic activity against HeLa cells, indicating their potential in anticancer studies.<sup>59</sup> The medicinal plant *S. irio* possesses powerful cytotoxic activity against cancer cell lines. However, further studies to understand their toxicity toward cells and their mode of action are required.

## 4. CONCLUSIONS

Approaches of nanoparticle production through various physical and chemical ways have their own shortcomings as they produce massive environmental pollution and lethal side effects. Therefore, the current trend of research encourages researchers all across the world to go for green synthesis of nanoparticles which is an easy, cost-effective, eco-friendly, well-controlled, and non-toxic approach. Green-synthesized *S. irio* ZnO NPs were found to possess high cytotoxic activity against human cancer cell lines (HepG2). Further studies are required for potential applications of *S. irio* Zn NPs in various diseases.

## AUTHOR INFORMATION

### Corresponding Authors

**Saima Maher** – Department of Chemistry, Sardar Bahadur Khan Women University, Quetta SXR6+85F Balochistan, Pakistan; [orcid.org/0000-0002-4269-6398](https://orcid.org/0000-0002-4269-6398); Email: [saimamaher@yahoo.com](mailto:saimamaher@yahoo.com)

**Muhammad Imran** – Department of Chemistry, Faculty of Science and Research Center for Advanced Materials Science (RCAMS), King Khalid University, Abha 61413, Saudi Arabia; Email: [imranchemist@gmail.com](mailto:imranchemist@gmail.com)

### Authors

**Shazia Nisar** – Department of Chemistry, University of Karachi, Karachi 72500, Pakistan

**Sania Muhammad Aslam** – Department of Chemistry, Sardar Bahadur Khan Women University, Quetta SXR6+85F Balochistan, Pakistan

**Farooq Saleem** – Faculty of Pharmacy, The University of Lahore, Lahore 82000, Pakistan

**Farida Behlil** – Department of Chemistry, Sardar Bahadur Khan Women University, Quetta SXR6+85F Balochistan, Pakistan

**Mohammed A. Assiri** – Department of Chemistry, Faculty of Science and Research Center for Advanced Materials Science (RCAMS), King Khalid University, Abha 61413, Saudi Arabia

**Arifa Nouroz** – Department of Chemistry, Sardar Bahadur Khan Women University, Quetta SXR6+85F Balochistan, Pakistan

**Nadra Naheed** – ICCBS, University of Karachi, Karachi 72500, Pakistan

**Zarina Azad Khan** – Department of Chemistry, Sardar Bahadur Khan Women University, Quetta SXR6+85F Balochistan, Pakistan

**Parveen Aslam** – Department of Chemistry, Sardar Bahadur Khan Women University, Quetta SXR6+85F Balochistan, Pakistan

Complete contact information is available at:

<https://pubs.acs.org/10.1021/acsomega.2c07621>

## Notes

The authors declare no competing financial interest.

## ACKNOWLEDGMENTS

The authors extend their gratitude to the Postdoc Scholarship (registration number (IsDB 600047711)), and M.A.A. extends his appreciation to the Deanship of Scientific Research at King Khalid University for funding this work through Large Group Research Project under grant number 34/43 and also acknowledges the Research Center for Advance Materials (RCAMS) at King Khalid University, Saudi Arabia for their valuable technical support.

## REFERENCES

- (1) Singh, A. K.; Viswanath, V.; Janu, V. effect of capping agents, structural, optical and photoluminescence properties of ZnO nanoparticles. *J. Lumin.* **2009**, *129*, 874–878.
- (2) Aljabali, A. A.; Al, Z.; Alzoubi, M. S.; Al-Batanyeh, L.; Obeid, K. M.; Tambwala, M. A. *Chemical engineering of protein cages and nanoparticles for pharmaceutical applications Nanofabrication for smart Nanosensor Application*; Elsevier, 2020, pp 415–433.
- (3) Al harbi, N. S.; Govindarajan, M.; Kadaikunnan, S.; Khaled, J. M.; Almanaa, T. N.; Alyahya, S. A.; Al-Anbr, M. N.; Gopinath, K.; Sudha, A. Nanosilver crystals capped with Bauhinia acuminata phytochemicals as new antimicrobials and mosquito larvicides. *J. Trace Elem. Med. Bio.* **2018**, *50*, 146–153.
- (4) Bello, B. A.; Khan, S. A.; Khan, J. A.; Syed, F. Q.; Mirza, M. B.; Shah, L.; Khan, S. B. Anticancer, antibacterial and pollutant degradation potential of silver nanoparticles from *Hyphaene thebaica*. *Biochem. Bioph. Res. Co.* **2017**, *490*, 889–894.
- (5) Hebbalalu, D.; Lalley, J. M.; Nadagouda, N.; Varma, R. S. Greener Techniques for the Synthesis of Silver Nanoparticles Using Plant Extracts, Enzymes, Bacteria, Biodegradable Polymers, and Microwaves. *ACS Sustain. Chem. Eng.* **2013**, *1*, 703–712.
- (6) Kuppusamy, P.; Yusoff, M. M.; Maniam, G. P.; Govindan, N. Biosynthesis of metallic nanoparticles using plant derivatives and their new avenues in pharmacological applications An updated report. *Saudi Pharm. J.* **2016**, *24*, 473–484.

- (7) Gopinath, K.; Kumaraguru, S.; Bhakayaraj, K.; Mohan, S.; Venkatesh, K. S.; Esakirajan, M.; Kaleeswaran, P.; Alharbi, N. S.; Kadaikunnan, S.; Govindarajan, M.; et al. Green synthesis of silver, gold and silver/gold bimetallic nanoparticles using the *Gloriosa superba* leaf extract and their antibacterial and antibiofilm activities. *Micro. Pathog.* **2016**, *101*, 1–11.
- (8) Pirtarighat, S.; Ghannadnia, M.; Baghshahi, S. Green synthesis of silver nanoparticles using the plant extract of *Salvia spinosa* grown in vitro and their antibacterial activity assessment. *J. Nanostruct. Chem.* **2019**, *9*, 1–9.
- (9) Prabakar, K.; Sivalingam, P.; Mohamed Rabeek, S. I.; Muthuselvam, M.; Devarajan, N.; Arjunan, A.; Karthick, R. M.; Suresh, M.; Wembonyama, J. P. Evaluation of antibacterial efficacy of phyto fabricated silver nanoparticles using *Mukia scabrella* (Musumukku) against drug resistance nosocomial gram negative bacterial pathogens. *Colloid. Surface B.* **2013**, *104*, 282–288.
- (10) Yugandhar, P.; Savithramma, N. Biosynthesis, characterization and antimicrobial studies of green synthesized silver nanoparticles from fruit extract of *Syzygium alternifolium* (Wt.) Walp. an endemic, endangered medicinal tree taxon. *Appl. Nanosci.* **2016**, *6*, 223–233.
- (11) Taid, T. R. A study on the medicinal plants used by the local traditional healers of Dhemaji district, Assam, India for curing reproductive health related disorders. *Advances in Applied Science Research* **2014**, *5*, 296–301.
- (12) Bhargava, M. T. Current Updates On *Sisymbrium irio* Linn: A Traditional Medicinal Plant. *Plant Archives* **2002**, *21*, 411–419.
- (13) Alsaffar, D. I. Investigation of the Main Alkaloid of London Rocket (*Sisymbrium irio* L) as a Wild Medicinal Plant Grown in Iraq. *Int. J. Pharm. Sci. Rev. Res.* **2016**, *56*, 279–281.
- (14) Hussain, M.; Waqas, H. M.; Raza, S. M.; Farooq, U.; Ahmed, M. M.; Majeed, A. Anti-cholinergic and Ca<sup>2+</sup>-antagonist mechanisms explain the pharmacological basis for folkloric use of *Sisymbrium irio* Linn. in gastrointestinal, airways and vascular system ailments. *Journal of ethnopharmacology* **2016**, *193*, 474–480.
- (15) Shah, S. R. *Pharmacognostic standardization and pharmacological study of Sisymbrium irio L*; AJRC, 2014, pp 241–253.
- (16) Bhargava, M. T.. *Current Updates On Sisymbrium irio Linn, A Traditional Medicinal Plant* *Plant Archives* 2021, Vol 21, pp 411–419.
- (17) Motaleb, M. *Selected medicinal plants of Chittagong hill tracts*; IUCN Bangladesh, 2011.
- (18) Rasool Hassan, B. Medicinal plants (importance and uses). *Pharmaceutical Anal Acta* **2012**, *3*, 2153.
- (19) Zereen, A.; Khan, Z.; Sardar, A. A. Ethnobotanical studies of wild herbs of central Punjab, Pakistan. *Bangladesh Journal of Plant Taxonomy* **2013**, *20*, 67–76.
- (20) Al-Massarani, S.; El Gamal, A. A.; Alam, P.; Al-Sheddi, E. S.; Al-Oqail, M. M.; Farshori, N. N. Isolation, biological evaluation and validated HPTLC-quantification of the marker constituent of the edible Saudi plant *Sisymbrium irio* L. *Saudi Pharmaceutical Journal* **2017**, *25*, 750–759.
- (21) Khalil, H. A. Phytochemical Analysis and in Vitro Antioxidant Properties of *Sisymbrium irio* L Growing in Saudi Arabia: A Comparative Study. *Res. J. Pharm., Biol. Chem. Sci.* **2017**, *8*, 2533.
- (22) Qureshi, M. GC-MS analysis of ethyl acetate fraction of leaf extract of London rocket weed for identification of possible antifungal constituents. *MYCOPATH* **2018**, *15*.
- (23) Al-Jaber, N. Phytochemical and biological studies of *Sisymbrium irio* L. Growing in Saudi Arabia. *Journal of Saudi Chemical Society* **2011**, *15*, 345–350.
- (24) Wiman, K. G.; Zhivotovsky, B. Understanding cell cycle and cell death regulation provides novel weapons against human diseases. *J. Intern. Med* **2017**, *281*, 483–495.
- (25) Pal, S. Nanoparticle: An overview of preparation and characterization. *J. of Applied Pharmaceutical Science* **2011**, *1*, 228–234.
- (26) Hasan, S. A review on nanoparticles: their synthesis and types. *Research Journal of Recent Sciences* ISSN 2015, 2502.
- (27) Brewer, G. J. Biological roles of ionic zinc. *Prog. Clin. Biol. Res.* **1983**, *129*, 35–51.
- (28) Al-saran, N.; Subash-Babu, P.; Al-Nouri, D. M.; Alfawaz, H. A.; Alshatwi, A. A. Zinc enhances CDKN2A, pRb1 expression and regulates functional apoptosis via upregulation of p53 and p21 expression in human breast cancer MCF-7 cell. *Environ. Toxicol. Pharmacol.* **2016**, *47*, 19–27.
- (29) Chasapis, C. T.; Loutsidou, A. C.; Spiliopoulou, C. A.; Stefanidou, M. E. Zinc and human health: An update. *Arch. Toxicol.* **2012**, *86*, 521–534.
- (30) Franklin, R. B.; Costello, L. C. The important role of the apoptotic effects of zinc in the development of cancers. *J. Cell. Biochem.* **2009**, *106*, 750–757.
- (31) Król, A.; Pomastowski, P.; Rafińska, K.; Railean-Plugaru, V.; Buszewski, B. Zinc oxide nanoparticles: Synthesis, antiseptic activity and toxicity mechanism. *Adv. Colloid Interface Science* **2017**, *249*, 37–52.
- (32) Sasidharan, A.; Chandran, P.; Menon, D.; Raman, S.; Nair, S.; Koyakutty, M. Rapid dissolution of ZnO nanocrystals in acidic cancer microenvironment leading to preferential apoptosis. *Nanoscale* **2011**, *3*, 3657–3669.
- (33) Hanley, C.; Layne, J.; Punnoose, A.; Reddy, K. M.; Coombs, I.; Coombs, A.; Feris, K.; Wingett, D. Preferential killing of cancer cells and activated human T cells using ZnO nanoparticles. *Nanotechnology* **2008**, *19*, 295103–103.
- (34) Zhang, Z.-Y.; Xiong, H. M. Photoluminescent ZnO nanoparticles and their biological applications. *Materials* **2015**, *8*, 3101–3127.
- (35) Alomari, G.; Al-Trad, B.; Hamdan, S.; Aljabali, A. A. A.; Al Zoubi, M. S.; Al-Batanyeh, K.; Qar, J.; Eaton, G. J.; Alkaraki, A. K.; Alshaer, W.; et al. Alleviation of diabetic nephropathy by zinc oxide nanoparticles in streptozotocin-induced type I diabetes in rats. *IET Nanobiotechnol* **2021**, *15*, 473–483.
- (36) Al-Trad, B.; Aljabali, A.; Al-Zoubi, M.; Shehab, M.; Omari, S. Effect of gold nanoparticles treatment on the testosterone-induced benign prostatic hyperplasia in rats. *International Journal of Nanomedicines* **2019**, *14*, 3145–3154.
- (37) Kumar, R.; Umar, A.; Kumar, G.; Nalwa, H. S. Antimicrobial properties of ZnO nanomaterials: A review. *Ceram.Int* **2017**, *43*, 3940–3961.
- (38) Agarwal, H.; Shanmugam, V. A review on anti-inflammatory activity of green synthesized zinc oxide nanoparticle: Mechanism-based approach. *Bioorg. Chem.* **2020**, *94*, 103423.
- (39) Kaushik, M.; Niranjana, R.; Thangam, R.; Madhan, B.; Pandiyarasan, V.; Ramachandran, C.; Oh, D. H.; Venkatasubbu, G. D. Investigations on the antimicrobial activity and wound healing potential of ZnO nanoparticles. *Appl. Surf. Sci.* **2019**, *479*, 1169–1177.
- (40) Mishra, P. K.; Mishra, H.; Ekielski, A.; Talegaonkar, S.; Vaidya, B. Zinc oxide nanoparticles: A promising nanomaterial for biomedical applications. *Drug Discov. Today* **2017**, *22*, 1825–1834.
- (41) Dagdeviren, C.; Hwang, S. W.; Su, Y.; Kim, S.; Cheng, H.; Gur, O.; Haney, R.; Omenetto, F. G.; Huang, Y.; Rogers, J. A. Transient, biocompatible electronics and energy harvesters based on ZnO. *Small* **2013**, *9*, 3398–3404.
- (42) Al-Dhabi, N.; Valan Arasu, M. Environmentally-Friendly Green Approach for the Production of Zinc Oxide Nanoparticles and Their Anti-Fungal, Ovicidal, and Larvicidal Properties. *Nanomaterials* **2018**, *8*, 500.
- (43) Zhou, P.; Chen, C.; Wang, X.; Hu, B.; San, H. 2-Dimensional photoconductive MoS<sub>2</sub> nanosheets using in surface acoustic wave resonators for ultraviolet light sensing. *Actuators A Phys* **2018**, *271*, 389–397.
- (44) Bisht, G.; Rayamajhi, S. ZnO nanoparticles: A promising anti-cancer agent. *Nanobiomedicine* **2016**, *3*, 9.
- (45) Kokhdan, E. Cytotoxic effect of methanolic extract, alkaloid and terpenoid fractions of *Stachys pilifera* against HT-29 cell line. *Research in Pharmaceutical Sciences* **2018**, *13*, 404–412.
- (46) Uikey, P. Review of zinc oxide (ZnO) nanoparticles applications and properties. *International Journal of Emerging Technology in Computer Science & Electronics* **2016**, *21*, 239.
- (47) Heera, P. Nanoparticle characterization and application: an overview. *Int. J. Curr. Microbiol. App. Sci* **2015**, *4*, 379–386.

(48) Vaseem, M. *ZnO nanoparticles: growth, properties, and applications. Metal oxide nanostructures and their applications*, 2010, pp 1–36.

(49) Mohan, A. Preparation of zinc oxide nanoparticles and its characterization using scanning electron microscopy (SEM) and X-ray diffraction (XRD). *Procedia Technology* **2016**, *24*, 761–766.

(50) Githinji, G. L. Quantitative Analysis of Total Phenolic Content in Avocado (*Persia Americana*) Seeds in Eastern Province of Kenya. *Chem. and Matl* **2013**, *3*, 48–51.

(51) Panchaksharam, K. V. Estimation of Phenolic Compounds Present in the Plant Extracts Using High Pressure Liquid Chromatography, Antioxidant Properties and its Antibacterial Activity. *Indian J. Pharm. Educ. Res.* **2018**, *52*, 321.

(52) Spiridon, I. *The total Phenolic Contents and anti-oxidant activity of Plant used in traditional Romanian herbal medicine & quot*; Central European Journal of Biology, 2011, p 390.

(53) Samshuddin, S. Determination of Total Phenolic Content and Total Antioxidant activity in locally consumed food stuff in Moodbidri, Karnataka, India & quot *Advance in Applied Science Research* Pelagia Research Library, 2011; Vol. 6, pp 99–102.

(54) Kamath, S. Determination of total phenolic content and total antioxidant activity in locally consumed food stuffs in Moodbidri, Karnataka, India. *Advances in Applied Science Research* **2015**, *6*, 99–102.

(55) Al-Jaber, N. A. Phytochemical and biological studies of *Sisymbrium irio* L. growing in Saudi Arabia. *J Saudi Chem Soc* **2011**, *15*, 345–350.

(56) Vohora, S. B.; Naqvi, S. A.; Kumar, I. Antipyretic, analgesic and antimicrobial studies on *Sisymbrium irio*. *Planta Med.* **1980**, *38*, 255–259.

(57) Qidwai, A.; Kumar, R.; Dikshit, A. Green synthesis of silver nanoparticles by seed of *Phoenix sylvestris* L. and their role in the management of cosmetics embarrassment. *Green. Chem Lett Rev* **2018**, *11*, 76–88.

(58) El Sherbiny, G. M.; Moghannem, S. A.; Sharaf, M. H. Antimicrobial activities and cytotoxicity of *Sisymbrium irio* L extract against multi-drug resistant bacteria (MDRB) and *Candida albicans*. *Int J Curr Microbiol App Sci* **2017**, *6*, 1–13.

(59) Rizwana, H.; Bokahri, N. A.; Alfarhan, A.; Aldehshish, H. A.; Alsaggabi, N. S. Biosynthesis and characterization of silver nanoparticles prepared using seeds of *Sisymbrium irio* and evaluation of their antifungal and cytotoxic activities. *Green Processing and synthesis* **2022**, *11*, 478–491.